ELSEVIER

Journal of Photochemistry and Photobiology A: Chemistry 151 (2002) 171–179

Journal of Photochemistry and Photobiology A:Chemistry

www.elsevier.com/locate/jphotochem

Novel TiO_2 CVD films for semiconductor photocatalysis

Andrew Mills [a,*], Nicholas Elliott [a], Ivan P. Parkin [b], Shane A. O'Neill [b], R.J. Clark [b]

[a] *Department of Pure and Applied Chemistry, University of Strathclyde, Thomas Graham Building, 295 Cathedral Street, Glasgow, G1 1XL UM, Scotland, UK*
[b] *Department of Chemistry, Christopher Ingold Laboratories, University College London, 20 Gordon Street, London WC1H 0AJ, UK*

Received 9 May 2002; accepted 17 May 2002

Abstract

A novel CVD film of titanium(IV) oxide has been prepared on glass, via the reaction of titanium(IV) chloride and ethyl acetate, using a CVD technique. The film is clear, very robust mechanically and comprised of a thin (24 nm) layer of nanocrystalline anatase titania that absorbs light of $\lambda < 360$ nm. The film is active in terms of photo-induced superhydrophilicity, and thus its water contact angle is reduced markedly (from 61 to 11°) upon irradiation with ultra-bandgap light. The film is also active photocatalytically and is able to destroy a deposited layer of stearic acid upon exposure to ultra-bandgap light. The photo-induced superhydrophilic and photocatalytic activities of this film are compared with those for one comprised of P25 particles.

Keywords: Titania; CVD; Photocatalyst; Superhydrophilicity; Stearic acid

1. Introduction

If the literature is anything to go by, semiconductor photochemistry continues to be the hottest subject in photochemistry, with publications in this area reaching the dizzy rate of one paper per day. Greatest interest in the subject has focused primarily on semiconductor photocatalysis (PC), in which the semiconductor photosensitizes a thermodynamically feasible reaction ([1], and references therein). Usually the latter reaction is the oxidation of an organic by oxygen, i.e.

$$\text{Organic} + O_2 \overset{h\nu \geq \text{bandgap energy}}{\underset{\text{semiconductor}}{\rightarrow}} CO_2 + H_2O + \text{mineral acids}$$

where mineral acids are generated if there are any hetero atoms, such as S, N and Cl, present in the original organic. Of possible greater significance are the recent findings of Fujishima et al., that some semiconductors also exhibit a photo-induced superhydrophilic effect (PSH), i.e. they are rendered more wettable by water after exposure to ultra-bandgap irradiation and that this process is reversible, albeit slowly, in the dark [2,3]. The photocatalytic activity and photo-induced superhydrophilicity of a semiconductor do not appear to be simply related. Thus, there are semiconductors which have a high PC activity but a negligible PSH activity, such as strontium titanate [4] and there are semiconductors, such as titanium(IV) oxide, i.e. TiO_2, that can exhibit either a high or low PC activity but usually a high PSH activity (vide infra).

In semiconductor PC ultra-bandgap light generates an electron–hole pair that can then either recombine or react with surface species. Thus, in reaction (1) sensitized by the semiconductor TiO_2, the photogenerated electrons reduce oxygen to water and the photogenerated holes mineralizes the organic. The latter process probably involves the initial oxidation of surface OH^- groups to hydroxyl radicals which then oxidise the organic and any subsequent intermediates [1]. What is most notable about PC as an organic destruction technique is the wide range of organics that can be mineralized; the list includes: aromatics, alkanes, alcohols, haloalkanes, dyes, insecticides and surfactants. What is most notable about TiO_2 is its chemical and biological inertness, high photocatalytic activity, photodurability, mechanical robustness and cheapness. In fact, TiO_2 is generally considered to be the best semiconductor photocatalyst available for PC at present. Of all the commercial sources of TiO_2, Degussa P25 TiO_2 has become widely recognized as the 'gold-standard', due to its high specific surface area (typically 50 $m^2\,g^{-1}$) and PC activity [1].

In semiconductor photo-induced superhydrophilicity [2,3], ultra-bandgap light generates an electron–hole pair that, once again can either recombine, or react with surface species. In the case of TiO_2, in the absence of any appreciable level of adsorbed competing species such as an organic, the surface species available for reaction appear to be Ti(IV)

* Corresponding author. Tel.: +44-141-548-2458; fax: +44-141-548-4822.
E-mail address: a.mills@strath.ac.uk (A. Mills).

1010-6030/02/$ – see front matter
PII: S1010-6030(02)00190-9

and bridging O^{2-} groups. As a consequence, hydrophilic surface Ti(III) species are generated, via the reduction of the Ti(IV) surface species by photogenerated electrons, and oxygen vacancies are generated, via the oxidation of the bridging O^{2-} species to oxygen by photogenerated holes. Adsorbed OH groups subsequently fill the oxygen vacancies and so increase the hydrophilic nature of the surface. The process is reversed, usually slowly, in the dark as the Ti(III) sites are oxidized back to Ti(IV) by ambient oxygen, and the vancancies filled by the O^{2-} generated as a consequence of this reaction. The rate of this reverse process can be enhanced by subjecting the film to ultrasound [5] or mechanical abrasion [6].

A great deal of early work into semiconductor PC was directed at the photomineralisation of organics dissolved in aqueous solution and usually employed the semiconductor in the form of a powder dispersion [1]. However, over time it has become increasingly apparent that most practical and possibly commercially viable manifestations of semiconductor PC, and/or superhydrophilicity, will utilize the semiconductor as a film. Recent work carried out by our group investigated the PC activity of P25 TiO_2 films on glass for the destruction of 4-chlorophenol [7]. The optimum, three coat, film, exhibited a PC activity that was only slightly less than that for an optimised dispersion of the same semiconductor photocatalyst. However, such films of P25 TiO_2, although not readily removed by washing, are mechanically frail and easily removed by rubbing with a cloth or the 3 M Scotch Tape test [8].

The mechanical frailty of semiconductor powder films for PC has helped promote recent research into the production and testing of nanocrystalline semiconductor films. Such films are produced almost exclusively by the sol–gel process, in which a metal complex, such as titanium isopropoxide, is reacted in a controlled manner with water. The hydrolysed product is then usually annealed, typically at 450 °C for 1 h, to produce a thin (usually 50–500 nm), nanocrystalline film of the semiconductor on the supporting substrate, usually glass [9]. Thus, in recent years, the sol–gel process has been used extensively to produce mainly anatase films of TiO_2 for semiconductor PC and superhydrophilicity research [1,3,9,10]. It remains to be seen if such a method of production is commercially viable in the long run.

Nanocrystalline films of titania can also be produced by the commercially more established process of chemical vapour deposition, CVD [11]. Yue and co-workers have used CVD to coat dense silica gel particles with TiO_2 [12]. The product is a readily-filtered powder photocatalyst that can be used in a flow system. However, as noted by Yue and co-workers, from the academic literature little work appears to have been conducted in this area with regard to CVD films of titania for PC [12]. This, observation is all the more striking given the recent announcement by the major glass manufacturer, Pilkington Glass, of the world's first light-activated, self-cleaning window glass, i.e. Activ^{TM}, the active ingredient of which is a 20 nm coat of titania deposited by an atmospheric pressure CVD technique, APCVD [13].

In this paper we describe the preparation, characterization and application of a thin, nanocrystalline film of titania on glass produced by a CVD technique. The photocatalytic and photo-induced superhydrophilic properties of this film are investigated and compared with those for a spin-coated film of Degussa P25 also on glass.

2. Experimental

2.1. Materials

Unless stated otherwise all materials used were purchased from Aldrich Chemicals, UK, and used as supplied. APCVD Titania thin films were deposited onto SiO_2-coated (29 nm) 3 mm float glass, i.e. barrier glass, as supplied by Pilkington Glass Plc. APCVD experiments were performed on 225 mm × 89 mm × 4 mm glass substrates using a cold wall APCVD reactor. The glass was cleaned prior to use by washing with distilled water, followed by isopropanol and finally petroleum spirits and drying in air. The glass substrate was heated using a graphite block containing three Whatman cartridge heaters; the temperature of the block was monitored using a Pt–Rh thermocouple. The APCVD rig was designed so that four separate gas lines could be used simultaneously; all gas lines were made of stainless steel, all 0.25 in. diameter, except for the inlet to the reaction chamber and the exhaust line from the reaction chamber which was 0.5 in. diameter. The nitrogen carrier gas was preheated to 150 °C by passing 2 m lengths of coiled stainless tubing inside a three zone tube furnace (7.5 ml min^{-1}). Gas temperatures were monitored in situ by Pt–Rh thermocouples. Titanium(IV) chloride, $TiCl_4$ (99.99%), was placed into a stainless steel bubbler, which was heated by a heating jacket to 68 °C and added to the gas stream by passing hot N_2 through the bubbler (0.2 ml min^{-1}). The oxygen source in this work, ethyl acetate, was introduced into the gas stream by passing hot N_2 through a bubbler set to 42 °C (0.2 ml min^{-1}). The overall gas flow rate into the reactor was 7.9 ml min^{-1}. The apparatus was baked at 150 °C for an hour prior to each run and the deposition time was 30 s. The substrate temperature was set at 600 °C. The coated substrates were cooled to 200 °C before removal from the graphite block. Coated substrates were handled and stored in air. The large substrates were cut into ca. 1 cm × 1 cm squares for analysis by SEM, XPS, Raman and UV studies. Squares 25 mm × 25 mm were used for X-ray diffraction, contact angle and PC tests. XPS, coupled with argon-ion bombardment, revealed that the films comprise a top layer of titania, ca. 28 nm thick. The UV–VIS spectrum of a typical APCVD titania coated barrier glass sample is illustrated in Fig. 1 and shows the film to be only slightly scattering at sub-bandgap wavelengths, such as 400 nm, and increasingly absorbing with decreasing wavelengths below the 360 nm, the approximate bandgap

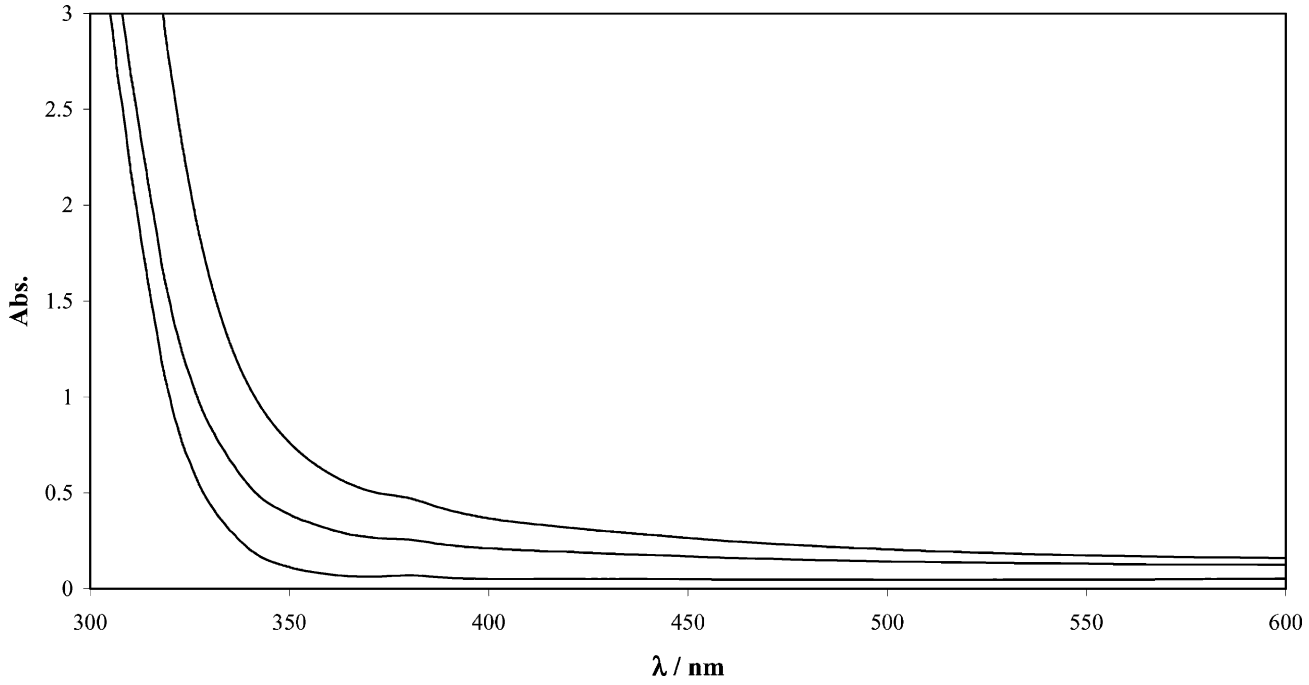

Fig. 1. UV–VIS absorption spectra of (from left to right) plain, CVD TiO_2 coated and P25 TiO_2 coated barrier glass, respectively.

of the nanocrystalline TiO_2 particles. The UV–VIS spectrum of plain barrier glass is also illustrustrated in Fig. 1 and shows it to be non-scattering, but also highly absorbing at wavelengths <310 nm, the normal UV cut-off for glass. Titania films produced by APCVD appeared mechanically very robust and thus could not be separated from its supporting glass substrate with repeated successive applications and removals of Scotch Tape (3 M, UK). In addition, the films could not be marked by a brass stylus or steel scalpel. XRD and Raman spectra showed that the titania films produced by APCVD were largely anatase, with no evidence for any rutile TiO_2. Unless stated otherwise, the films were washed and wiped clean with methanol, dried in an oven at 80 °C, and stored, at least overnight, in the dark prior to use.

The Degussa P25 TiO_2 films on glass substrates were cast by spin-coating 25 mm × 25 mm × 3 mm squares of barrier glass (Pilkington Glass, UK) with a 5 (wt.%/v) aqueous slurry of Degussa P25 TiO_2. The P25 slurry was deposited by dropping pipette until the whole surface of the glass surface was covered and then spun at 2900 rpm for 30 s using a model 4000-1 spin coater (Electro-Micro Systems). The films were then washed with distilled water and dried, first in an air stream and then in an oven at 80 °C for 1 h. The films were always stored, at least over night, in the dark before use and, unless stated otherwise, used without further treatment. Films produced by this method were stable to repeated washing with water but not to mechanical abrasion. Profilometry revealed that the films had a typical thickness of 90 ± 10 nm. The UV–VIS spectrum of a spin-coat film of Degussa P25 TiO_2 on glass is illustrated in Fig. 1 and shows the film to be highly scattering at sub-bandgap wavelengths, such as 400 nm, but also strongly absorbing at wavelengths below the 380 nm, the approximate bandgap of the microcrystalline TiO_2 particles. XRD and Raman spectra confirmed that the titania film was a mixture of primarily anatase (80%) and some rutile (20%). Although Degussa P25 TiO_2 comprises fundamental particles that are nanocrystalline, i.e. typically 30 nm, the latter form an irreducible complex of primary aggregates typically 0.1 μm in diameter and, as a consequence it appears more appropriate to refer to P25 TiO_2 films as near-microcystalline, rather than nanocrystalline [1,8].

3. Methods

UV–VIS absorption spectra were recorded using a Lambda 20 UV–VIS spectrophotometer (Perkin-Elmer, UK). Contact angles were measured using an FTA200 contact angle instrument (supplied by Camtel, UK). This instrument allows the vertical deposition of a 14 μl water droplet onto the substrate under test via a 100 μl syringe coupled to a 27 gauge needle with a 90° bevel tip. The changes in shape of the droplet that occur after it makes contact with the substrate under test are monitored using a combination of a white light source, prism and CCTV in a plane perpendicular to that of its the delivery, i.e. horizontally. The resulting profile images of the water droplet are recorded and then analysed using a computer and proprietary FTA software. Using this data contact angle versus time plots were generated and showed that for all tested substrates the droplet is stable and the contact angle remains unchanged for many minutes within 30 s of the drop falling

on the substrate under test. As a result, contact angles reported in this paper refer to a water droplet 30 s after the drop has made contact with the substrate under test. In this work ultra-bandgap irradiation of the films under test were carried out using two 8 W, 254 nm germicidal lamps (BDH, UK) for 30 min.

In the study of the photocatalytic activity of the various TiO_2 films, stearic acid was used as the organic material to be mineralized [8,14–16]. In order to coat each of the films under test with an initial layer of stearic acid, three successive 1.0 ml lots of a 10^{-3} mol dm^{-3} stearic acid in methanol solution were applied, with 5 min drying in an oven at 80 °C between each addition. Each final coated film was dried in an oven at 80 °C for 10 min, allowed to cool and then used directly. The infra-red spectrum of the film before and after the addition of the stearic acid layer was recorded using a 1600 FT-IR (Perkin-Elmer, UK). The same instrument was used to record the FT-IR spectrum of the film as a function of time of irradiation with ultra-badgap light. The FT-IR spectrum v 2.00 software (Perkin-Elmer, UK) allowed the integrated area under the stearic acid peaks, over the range 2700–3000 cm^{-1}, to be determined for each FT-IR spectrum recorded for a stearic acid covered film. A typical stearic acid layer on any of the test substrates, e.g. glass or CVD TiO_2 film on glass, had an integrated absorbance over this range of 8.0 cm^{-1}, corresponding to ca. 2.5×10^{16} molecules cm^{-2} [8].

In the study of the photocatalytic activities of the various films the irradiation source was either six 8 W blacklight bulbs (i.e. 365 ± 20) nm or six 8 W germicidal lamps (i.e. 254 nm), each set in a half cylinder unit, which had a backing aluminium reflector [17]. In either case the sample under test was placed on the bench and the irradiation unit placed 10 cm vertically overhead. This system, coupled with periodic analysis of the samples under test by FT-IR, allowed the concentration of stearic acid on each test sample to be monitored as a function of irradiation time. The light outputs from the two illumination sources, i.e. BLB and germicidal lamps, were determined by ferrioxalate actinometry [18] to be 7.6×10^{17} photons cm^{-2} min^{-1} (ca. 6.9 mW cm^{-2}) and 4.6×10^{17} photons cm^{-2} min^{-1} (ca. 6.0 mW cm^{-2}), respectively.

4. Results and discussion

4.1. Photo-induced superhydrophilicity

The contact angle of a water droplet was measured 30 s after its deposition onto (a) plain, (b) P25 TiO_2 coated and (c) CVD TiO_2 coated glass, respectively. The process was then repeated after these three types of glass had been exposed to 30 min of 254 nm light (2.0 mW cm^{-2}). The profile images of these water droplets are illustrated in Fig. 2 and were used to calculate the water–glass contact angles for each of the films reported in Table 1. The water droplet profile images in Fig. 2 provide a dramatic illustration of the photo-induced superhydrophilic effect. Thus, the water droplets on plain barrier glass, before and after irradiation appear very similar, as expected for a non-coated piece of glass. In contrast, the images for glass coated with P25, or CVD, TiO_2 show the contact angle to be reduced very greatly upon exposure of the films to ultra-bandgap irradiation. Thus, the water contact angle for the P25 TiO_2 film, already low (8°) before irradiation, is reduced to 0° after bandgap irradiation. To our knowledge, the water contact angle for a film of Degussa P25 TiO_2, or any other film comprising near-microcrystalline aggregated TiO_2 powder particles, has never been reported before. The results show photo-induced superhydrophilicity is not the preserve of smooth, robust nanocrystalline films of TiO_2, but instead can be readily demonstrated for films of coars, fragile near-microcrystalline aggregated forms of TiO_2, such as Degussa P25. The images in Fig. 2, and the results in Table 1, show that the CVD TiO_2 film also exhibits marked photo-induced superhydrophilicity, with its water contact angle dropping from 61 to 11° upon exposure to the ultra-bandgap light.

Table 1
Water contact angle data, before and after irradiation, and stearic acid photodestruction data

Sample	Contact angle pre-irradiation (°)	Contact angle[a] post-irradiation	Initial rate of photodegradation[c] (10^{13} molecules cm^{-2} min^{-1})		δ[b] (10^{-5} molecules per photon)	
			365 nm	254 nm	365 nm	254 nm
P25	8	Nil	8.34	104.00	11	228
CVD TiO_2	61	11	0.23	2.01	0.3	4.4
Barrier	33	19	0.03	0.53	0.04	1.2
P25[c]	–	–	–	–	146	270
Sol–gel[c]	–	–	–	–	18	220
Sol–gel[d]	–	–	–	–	9.9	–

[a] In all contact angle work the samples were irradiated with 2 × 8 W 254 nm germicidal lamps for 30 min.
[b] In all stearic acid work illumination with 365 or 254 nm light were conducted using 6 × 8 W black light bulbs and 6 × 8 W germicidal lamps, respectively.
[c] Formal quantum yield efficiency data reported by Heller and co-workers for a 300 nm thick TiO_2 sol–gel film [21] and a ca. 1.3 μm film of Degussa P25 TiO_2 [8].
[d] Formal quantum yield efficiency data reported by Minabe et al. for a 400 nm thick TiO_2 sol–gel film [16].

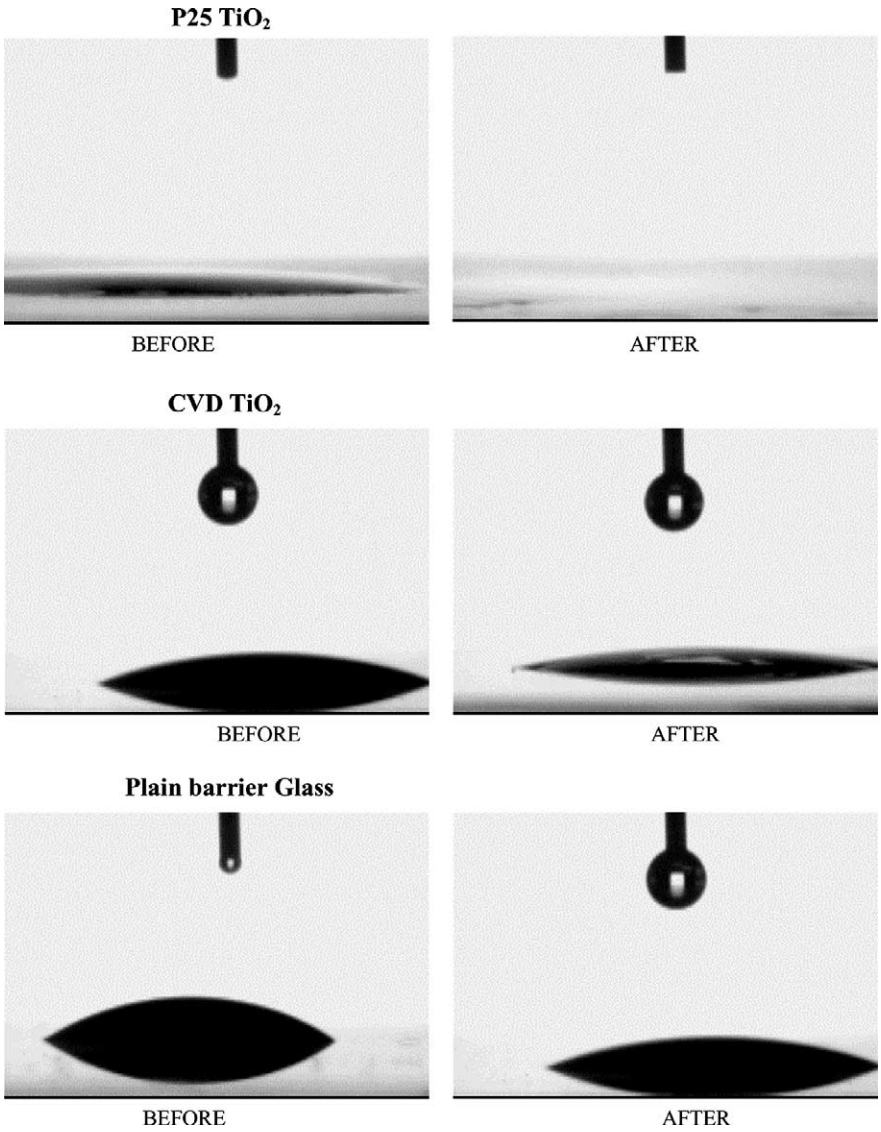

Fig. 2. CCTV water droplet profiles, recorded 30 s after touching the surface, before and after illumination with 365 nm (BLB) light for 30 min. The films tested were, from top to bottom, P25 TiO_2 coated, CVD TiO_2 coated and plain barrier glass, respectively.

In all cases this phenomena appeared reversible, by storing the films in the dark over a 24–48 h period, and repeatable.

4.2. Photocatalytic activity

A measure of photocatalytic activity that is commonly employed in semiconductor PC to assess the activities of films is the rate of photodestruction of stearic acid ($CH_3(CH_2)_{16}CO_2H$) [8,14–16], i.e.

$$CH_3(CH_2)_{16}CO_2H + 26O_2 \overset{h\nu \geq \text{bandgap energy}}{\underset{\text{semiconductor}}{\rightarrow}} 18CO_2 + 18H_2O$$

Note that this overall process involves the transfer of a 104 electrons. The melting point of stearic acid is markedly above room temperature, i.e. 69.3 °C, and, as a consequence, stearic acid forms solid films when deposited, usually by a spin- or dip-coating technique, on the substrate under test. The photocatalytic destruction of such solid compounds are of practical interest since they provide a reasonable model compound for the type of solid organic film that deposits on indoor or enclosed glass surfaces, such a kitchen window or a light cover in a road tunnel. The destruction of stearic acid is readily monitored by FT-IR absorbance spectroscopy, through the disappearance of the peak at 2957.5 cm^{-1}, due to the asymmetric in-plane C–H stretching mode of the CH_3 group, and the peaks at 2922.8 cm^{-1} and 2853.4 cm^{-1}, due to the asymmetric and symmetric C–H stretching modes of the CH_2 group, respectively [14]. In this work the integrated area under all these peaks was measured and used to calculate the surface concentration of stearic acid as a function of irradiation time.

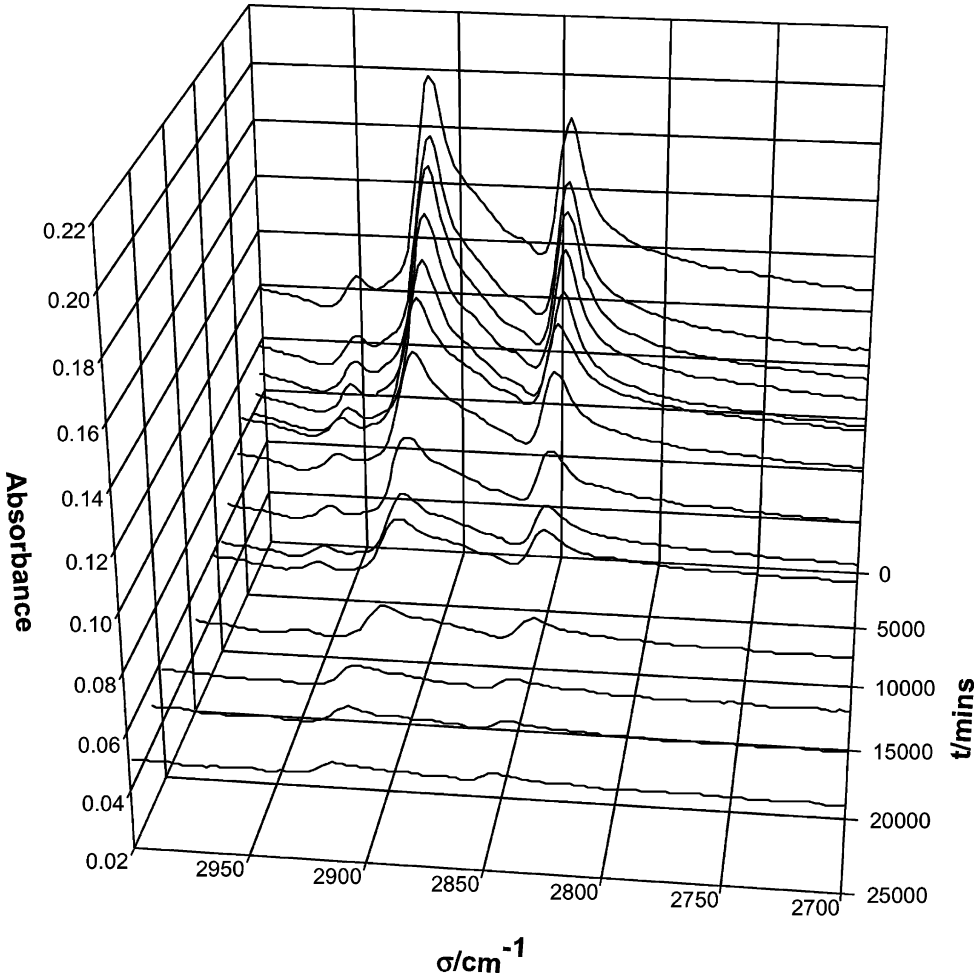

Fig. 3. FT-IR absorbance versus wavenumber, σ, specta, recorded for a CVD TiO_2 on glass film coated with stearic acid, as a function of irradiation time. The irradiation source comprised six 8 W blacklight bulbs, i.e. 365 ± 20 nm light.

Fig. 3 illustrates the observed variation in the FT-IR absorbance spectrum of a typical stearic acid film, deposited on a CVD TiO_2 coated sample of barrier glass, as a function of time of irradiation with ultra-bandgap (365 nm) light. From the data in Fig. 3 it is clear that the stearic acid peaks disappear, albeit slowly, with ultraband gap irradiation, as expected from Eq. (2). Also illustrated in Fig. 3, is the concomitant decrease in background absorbance, at wavenumbers where the stearic acid does not absorb IR, such as 2750 cm^{-1}, with increasing irradiation time. This latter observation is not surprising given that this background absorbance is due to scattering of the interrogating incident IR radiation by the stearic acid film; the thicker the film the greater the scattering and the higher the apparent absorbance. Thus, as the irradiation proceeds, and the stearic acid is destroyed, the film becomes less scattering, i.e. clearer, and the background absorbance decreases. Not too surprisingly, the actual IR absorbance, due to the stearic acid peaks at 2957.5, 2922.8 and 2853.4 cm^{-1}, and the apparent IR absorbance, due to scattering, appear to be directly related. Thus, it appears possible to monitor the destruction of stearic acid, or any other solid organic film coating, spectrophotometrically at wavelengths where the solid organic film either absorbs and/or scatters the incident monitoring light. This feature may be particularly useful in studies carried out on TiO_2 films on conducting glass, since the conducting glass is usually opaque to IR, but not visible irradiation.

FT-IR absorption spectra of a TiO_2 CVD film on glass were recorded at regular intervals upon its irradiation with ultra-bandgap (365 nm) light. Results were of the kind illustrated in Fig. 3 and allowed the calculated integrated area under the absorption peaks due to stearic acid to be measured as a function of irradiation time. The process was repeated for a P25 TiO_2 film on barrier glass and for barrier glass alone and the normalized results are illustrated in Fig. 4. The absorbance versus time profile for the barrier glass illustrated in Fig. 4 shows that it is unable to photocatalyse the destruction of stearic acid. This particular absorbance versus time profile also shows that the covering film of stearic acid is photochemically stable upon prolonged exposure to UVA, i.e. 365 nm, light. As indicated by the results illustrated in Fig. 3 and now further ratified by the normalized

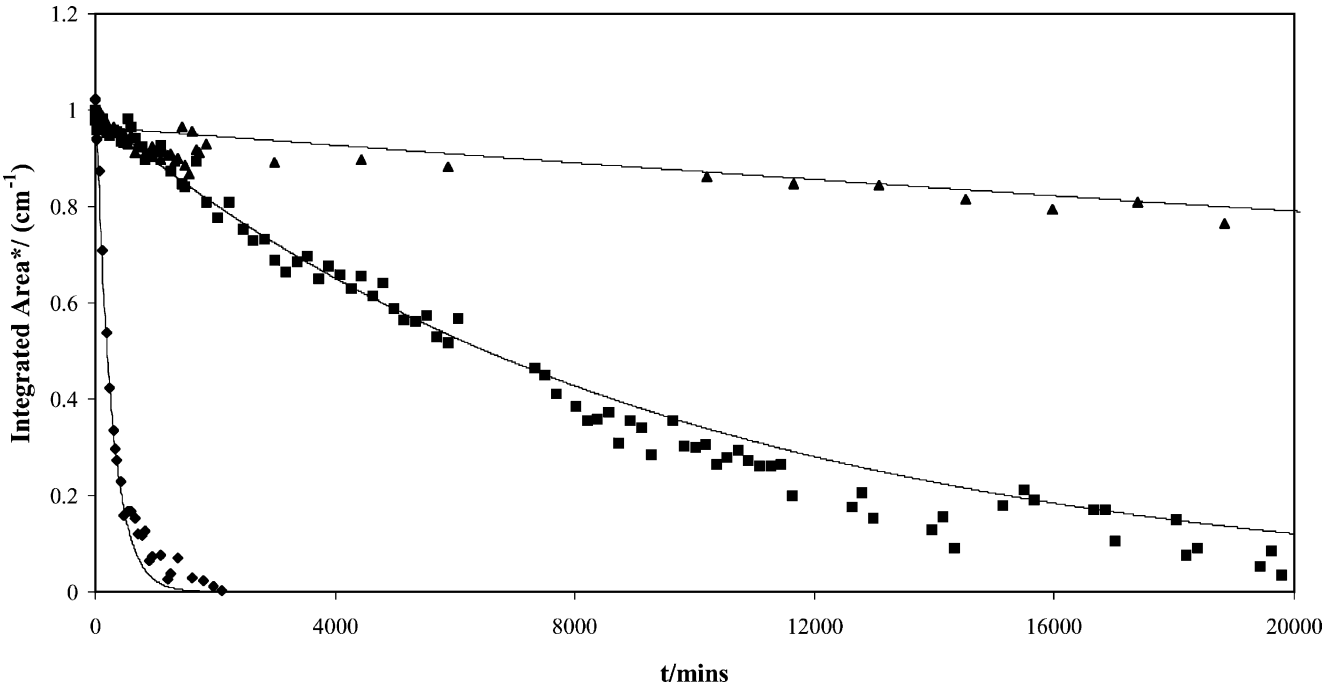

Fig. 4. Normalised integrated area, i.e. integrated area*, vs. irradiation time profiles for (from top to bottom) plain, CVD TiO_2 coated and P25 TiO_2 coated barrier glass, respectively. The irradiation source comprised six 8 W blacklight bulbs, i.e. 365 ± 20 nm light.

absorbance verus time profile in Fig. 4, a CVD TiO_2 coating on barrier glass renders the film photocatalytically active for the removal of stearic acid, via. reaction (2). Also striking about the results illustrated in Fig. 4 is the apparent much greater photocatalyic activity exhibited by the thin Degussa P25 film on barrier glass towards reaction (2) than that shown by the CVD TiO_2 film. The results illustrated in Fig. 4 were used to calculate the initial rates of stearic acid photodegradation reported in Table 1 from which it appears that the initial rate of destruction of stearic acid, at 365 nm, is ca. 36 times greater for a P25 TiO_2 film compared to that for a CVD TiO_2 film and that, under the same illumination conditions, the rate of destruction of stearic acid on barrier glass is negligible.

Although the Degussa P25 film is nominally ca. three-times thicker than the CVD TiO_2 film, it is less densely packed and, as a consequence although it has a higher absorbance (0.48 compared with 0.22) at 365 nm, it is not three times higher as might initially be expected. In addition, based on these two absorbances, it would appear that the Degussa P25 TiO_2 film will absorb ca. 67% of the incident 365 nm light compared to 40% by the CVD TiO_2 film. This difference is small and cannot be used to account for the striking differences in initial rate as indicated by the results in Table 1. In fact, the discrepancy between the initial rates for the two films and the amounts of light absorbed is further compounded when it is recognized that a Degussa P25 TiO_2 film is comprised of large, aggregated, highly scattering particles. As a result, it is likely that the ratio of the amount of ultra-bandgap light actually absorbed by the P25 and CVD TiO_2 films will be less than the projected approximate value of 67:40. Thus, it appears that the major difference in the initial rates of photocatalytic destruction of stearic acid by P25 and CVD TiO_2 is not simply due a difference in the amount of UV light absorbed. Instead, it appears that P25 TiO_2 is simply much more active photocatalytically than TiO_2 produced by the CVD method. Other experiments indicate that nanocrystalline films generated by the sol–gel process are also markedly less active than Degussa P25, but similar in activity to CVD TiO_2 films of the same thickness. Thus, the much lower activity of the CVD TiO_2 films may reflect a general, intrinsic property of nanaocrystalline TiO_2, when compared to TiO_2 powder particles comprising near microcrystalline aggregates, such as those found in films of Degussa P25. This general feature may simply be due to fundamental particle size. In CVD and sol–gel films the fundamental particle size is usually ca. 3–5 nm [8], whereas in Degussa P25 it is much bigger, i.e. 30 nm [7]. The smaller the fundamental particle size the more likely the greater the density of edges and defects that can act as electron–hole recombination sites; a process that is considered the major efficiency-lowering process in semiconductor PC [1]. The general feature of higher photocatalytic activity with larger fundamental particle size may also be due in some part to the amount of highly defective amorphous material present. Thus, the smaller the fundamental particle size in a film the more likely the presence of a significant fraction of highly defective amorphous material. Thus, some nanocrystalline production methods may produce photocatalyst films that exhibit a much higher

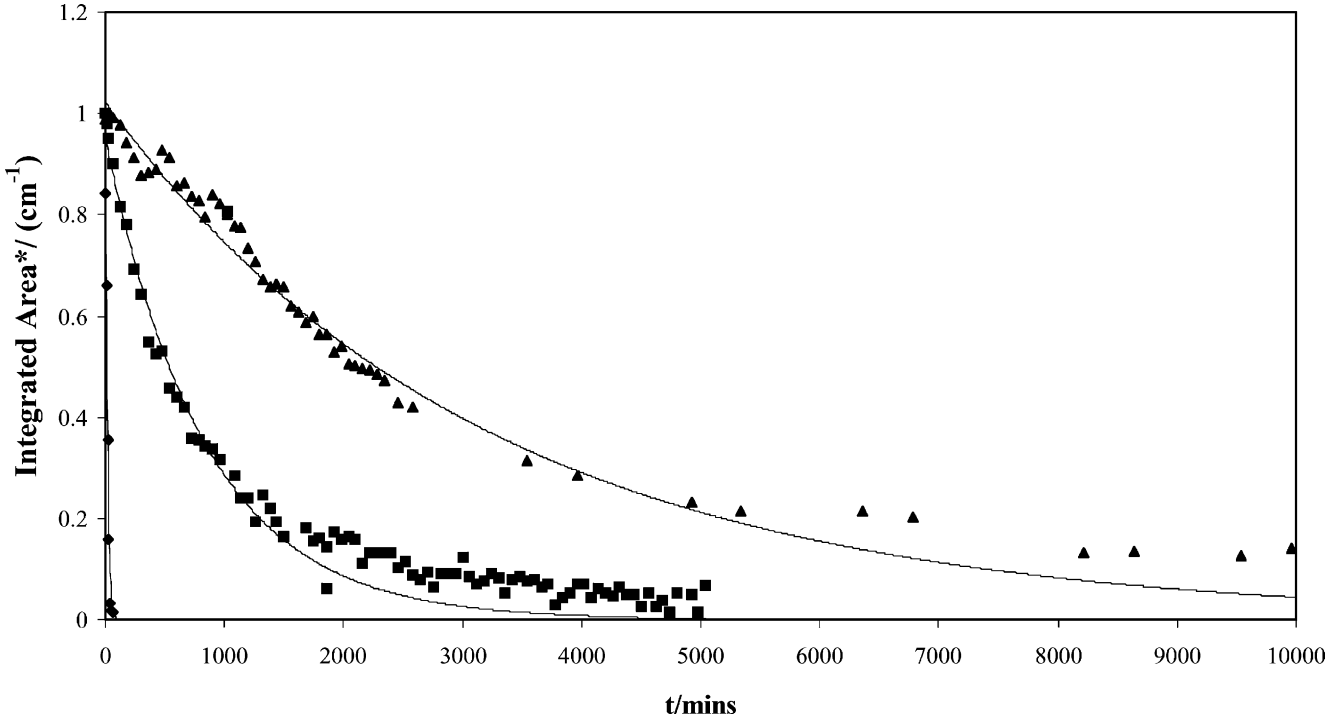

Fig. 5. Normalised integrated area, i.e. integrated area*, vs. irradiation time profiles for (from top to bottom) plain, CVD TiO_2 coated and P25 TiO_2 coated barrier glass, respectively. The irradiation source comprised six 8 W germicidal lamps, i.e. 254 nm light.

activity than other production methods, simply because the fraction of associated amorphous material is less. Further work is required in this area to resolve the question why films of nanocrystalline CVD, and sol–gel, TiO_2 appear markedly less active that films of Degussa P25 TiO_2?

The FT-IR absorption spectra of a TiO_2 CVD film on glass were also recorded at regular intervals upon its irradiation with ultra-bandgap UVC, 254 nm, light. Once again the results allowed the calculation of the integrated area under the absorption peaks due to stearic acid to be calculated as a function of irradiation time. The process was repeated for a P25 TiO_2 film on barrier glass and for barrier glass alone and the normalized results are illustrated in Fig. 5. Unlike irradiations performed using UVA light, the results illustrated in Fig. 5 show that stearic acid is slowly but surely decomposed by 254 nm light, even on plain barrier glass. However, the results in Fig. 5 also show that the rate of stearic acid removal is greatly enhanced when a TiO_2 CVD film is present and that the enhancement is even more dramatic when a film of Degussa P25 TiO_2 is present. As before, the results illustrated in Fig. 5 were used to calculate the initial rates of stearic acid photodegradation and these are reported in Table 1. From the values of the initial rates in Table 1 it appears that the initial rate of photodestruction of stearic acid, using 254 nm light, is ca. 52 times greater for P25 TiO_2 compared to that for the CVD TiO_2 film; under the same illumination conditions the rate of destruction of stearic acid on barrier glass is significant but ca. 200 times less than that for the P25 TiO_2 film.

In order to make some useful comparisons between the two sets of initial rates recorded for the various films using 365 and 254 nm ultra-bandgap light, the initial rates need to be corrected for the amount of incident light falling onto the sample. This, correction is effectively achieved through the calculation of the formal quantum efficiency of the system, δ, where formal quantum efficiency is defined as [1,19]:

$$\delta = \frac{\text{rate of photoreaction (molecules s}^{-1})}{\text{incident light intensity (photons s}^{-1})}$$

For any photochemical process, the formal quantum efficiency is, by definition, ≤quantum yield [15]. Using the initial rate data in Table 1, and values for the light intensities measured by chemical actinometry, the values of δ for the removal of a stearic acid film, using 365 and 254 nm irradiation light, were calculated for each of the glass substrates tested and the results are given in Table 1. The values in Table 1 show that the photocatalytic process, i.e. reaction (2), is apparently very inefficient for all the films tested, since the values of δ lie in the range (228–0.3) $\times$ 10^{-5} molecules per photon, although, it should be remembered that the complete mineralisation of stearic acid is a 104 electron process. The marked increase in initial rate and formal quantum efficiency for both the CVD and Degussa P25 TiO_2 films on changing from a 365 to 254 nm irradiation light source can be attributed largely to the greater absorption coefficient for TiO_2 at 254 nm compared to 365 nm. Thus, the reciprocal

length, α, for TiO_2 is estimated to be ca. $0.5 \times 10^5\ cm^{-1}$ at 365 nm and $5.1 \times 10^5\ cm^{-1}$ at 254 nm [7,20].

The destruction of stearic acid has been reported by others for both P25 and sol–gel films of TiO_2 and some of the results are given in Table 1 [8,16,21]. The formal quantum efficiencies reported by Heller and co-workers for a 1.3 μm thick film of Degussa P25 TiO_2 are not too out of line with those reported in this paper for a 0.1 μm thick film of the same material [8]. Indeed, for 254 nm irradiation light, the values of δ for the two films are very similar, i.e. 270×10^{-5} and 228×10^{-5} molecules per photon for the two P25 TiO_2 films, respectively. This similarity in δ values might be expected as both films will absorb most of the incident 254 nm UV light, due to the high value of the reciprocal length of TiO_2 at this wavelength.

In contrast, Heller and co-workers report that the value of δ for a P25 TiO_2 photocatalytic film for reaction (2) is only slightly reduced if 365 nm light, rather than 254 nm light is used, (dropping from 270×10^{-5} to 146×10^{-5} molecules per photon) [8], whereas in this work for the same change in excitation wavelength the change in the value of δ was found to be significant, i.e. from 228×10^{-5} to 11×10^{-5} molecules per photon. However, this difference can be largely attributed to the thickness of the respective semiconductor films. Thus, in the work of Heller and co-workers the P25 TiO_2 film was 1300 nm thick, and as such will absorb most of any incident 365 nm light, as well as any the 254 nm light [8]. In contrast, in this work the P25 TiO_2 film was 90 nm thick, and thus, although still an excellent absorber of 254 nm light, due to the high reciprocal length of TiO_2 at this wavelength, the amount of 365 nm light absorbed by this film will be much less.

In contrast to the similarities in the studies of reaction (2), sensitized by P25 TiO_2 films, from the results contained in Table 1 it is apparent that TiO_2 sol–gel films appear much more photocatalytically active than CVD TiO_2 [16,21]. Indeed, the values of δ for the sol–gel TiO_2 films are similar to that found in this work for a 90 nm film of Degussa P25. However, in both cases the sol–gel films used were much thicker (300–400 nm) than either the Degussa P25 (90 nm) or CVD (25 nm) TiO_2 films used in this work [16,21]. Thus, a simple comparison of δ values can be misleading if the films are not of the same thickness. Obviously, some of the apparent higher photocatalytic activities of the two sol–gel TiO_2 films compared with the CVD TiO_2 films listed in Table 1 will be due to greater absorbance of the incident 365 nm irradiation. Further work is required to ascertain if this difference in activity is solely due to film thickness, or whether sol–gel TiO_2 films are just inherently markedly more active as photocatalysts in reaction (2) than CVD TiO_2 films, possibly due to the production of a smaller fraction of efficiency-lowering amorphous material.

5. Conclusion

Robust, thin nanocrystalline films of titania on glass can be produced by an atmospheric pressure CVD technique. Less robust, thin films of P25 TiO_2 can also be produced and used as a comparison. All films are active both in terms of photo-induced superhydrophilicity and PC, although the P25 films perform markedly better than the CVD TiO_2 films. The results compare quite well with those reported previously by other for P25 TiO_2 and sol–gel films. The advantages of nanocrystalline TiO_2 films over the near-microcrystalline TiO_2 films of Degussa P25 is robustness and optical clarity. These two features render the films commercially viable, despite their low photoactivities. Further work is required to see if highly photoactive nanocrystalline TiO_2 films can be prepared by either a CVD or sol–gel technique to challenge the coveted position of Degussa P25 TiO_2 as one of the most photoactive forms of titania.

References

[1] A. Mills, S. LeHunte, J. Photochem. Photobiol. A: Chem. 108 (1997) 1.
[2] A. Fujishima, R. Wang, K. Hashimoto, T. Watanabe, M. Chikuni, E. Kojima, A. Kitamura, M. Shimohigoshi, Adv. Mater. 10 (1998) 135.
[3] A. Fujishima, T.N. Rao, D. Tryk, J. Photochem. Photobiol. C: Photochem. Rev. 1 (2000) 1.
[4] M. Miyauchi, A. Nakajima, A. Fujishima, K. Hashimoto, T. Watanabe, Chem. Mater. 12 (2000) 3.
[5] N. Sakai, R. Wang, A. Fujishima, T. Watanabe, K. Hashimoto, Langmuir 14 (1998) 5918.
[6] M. Kamei, T. Mitsuhashi, Surf. Sci. 463 (2000) L609.
[7] A. Mills, J. Wang, J. Photochem. Photobiol. A: Chem. 118 (1998) 53.
[8] Y. Paz, Z. Luo, R. Rabenberg, A. Heller, J. Mater. Res. 10 (1995) 2842.
[9] N. Negishi, T. Iyoda, K. Hashimoto, A. Fujishima, Chem. Lett. (1995) 841.
[10] I. Sopyan, M. Watanabe, S. Murasawa, K. Hashimoto, A. Fujishima, Chem. Lett. (1996) 69.
[11] S. Seifried, M. Winterer, H. Mahn, Chem. Vap. Dep. 6 (2000) 239.
[12] Z. Ding, X. Hu, G.Q. Lu, P.-L. Yue, P.F. Greenfield, Langmuir 16 (2000) 6216.
[13] http://www.pilkington.com.
[14] P. Sawunyama, L. Jiang, A. Fujishima, K. Hashimoto, J. Phys. Chem. B 101 (1997) 1103.
[15] P. Sawunyama, A. Fujishima, K. Hashimoto, Langmuir 15 (1999) 3551.
[16] T. Minabe, D.A. Tryk, P. Sawunyama, Y. Kikuchi, K. Hashimoto, A. Fujishima, J. Photochem. Photobiol. A: Chem. 137 (2000) 53.
[17] A. Mills, S. Morris, J. Photochem. Photobiol. A: Chem. 71 (1993) 75.
[18] J.G. Calvert, J.N. Pitts, Photochemistry, Wiley, New York, 1967, p. 783.
[19] T. Watanabe, T. Takizawa, K. Honad, J. Phys. Chem. 81 (1977) 1845.
[20] A. Hagfeldt, M. Graetzel, Chem. Rev. 95 (1995) 49.
[21] S. Sitkiewitz, A. Heller, New J. Chem. 20 (1996) 233.